J Sol-Gel Sci Technol (2016) 78:285–292
DOI 10.1007/s10971-015-3941-8

ORIGINAL PAPER: NANO-STRUCTURED MATERIALS (PARTICLES, FIBERS, COLLOIDS, COMPOSITES, ETC.)

Biosynthesis of silver nanoparticles using *Lantana camara* flower extract and its application

Brajesh Kumar[1] · Kumari Smita[1] · Luis Cumbal[1]

Received: 28 October 2015 / Accepted: 14 December 2015 / Published online: 30 December 2015

Abstract Search of new pigment for the green synthesis of nanoparticles has emerged new scope for the chemist. In this report, we describe the synthesis of silver nanoparticles (AgNPs) using notorious weed, *Lantana camara* L. flower extract. The AgNPs were characterized by visual, UV–visible spectrophotometer, transmission electron microscopy (TEM), dynamic light scattering and X-ray diffraction (XRD). UV–visible spectroscopy showed surface plasmon resonance at 470 nm clearly reveals the formation of AgNPs. TEM analysis confirmed that the AgNPs are spherical and 33 ± 5 nm average sized. XRD analysis reveals the formation of pure silver metal with face-centered cubic symmetry and confirms crystalline nature. The AgNPs showed significant antioxidant efficacy at different time intervals against 1,1-diphenyl-2-picrylhydrazyl and photocatalytic activities by the degradation of the methylene blue. From the results obtained, it is suggested that surface-modified AgNPs could be used effectively in future biotechnology concerns.

Graphical Abstract

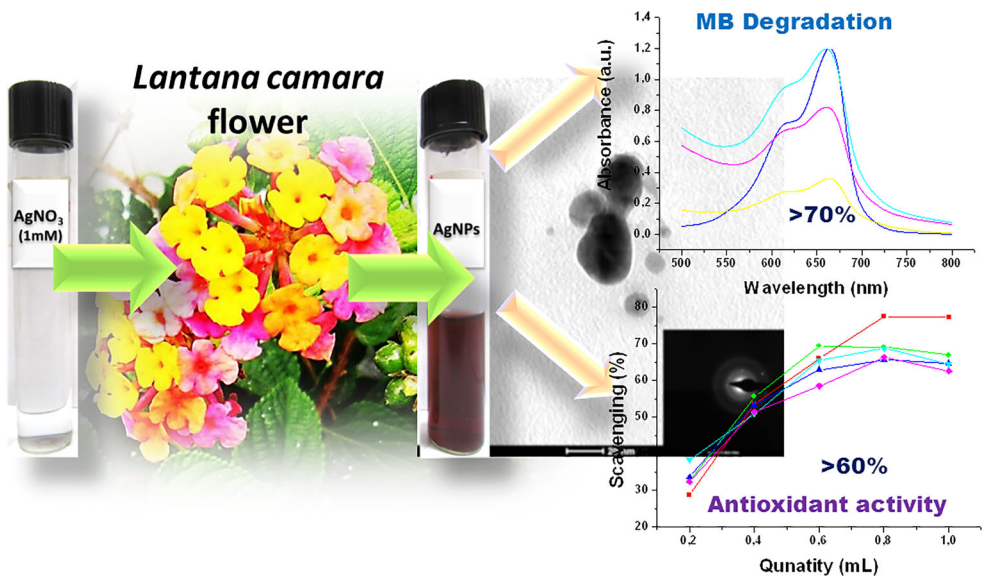

✉ Brajesh Kumar
krmbraj@gmail.com

[1] Centro de Nanociencia y Nanotecnologia, Universidad de las Fuerzas Armadas ESPE, Av. Gral. Rumiñahui s/n, P.O. BOX 171-5-231B, Sangolqui, Ecuador

Keywords Biosynthesis · *Lantana camara* · Silver nanoparticles · TEM · DPPH · Antioxidant · Methylene blue · Photocatalyst

1 Introduction

The development of an economically and ecologically favorable technique for the synthesis of nanoparticles is a great challenge in nanotechnology. Nanostructured materials or nanomaterials have one spatial dimension in the range of 1–100 nm [1] which includes thin films and bulk materials made of nanoscale building blocks and consisting of nanoscale structures, e.g., nanorods, nanowires and nanoparticles (NPs). In the past few years, there has been much attention in using silver nanoparticles (AgNPs) in new technologies, due to the surface plasmon resonance (SPR) in the visible region, which can be easily monitored by UV–visible spectrophotometer. The applications of AgNPs in the field of medicine, optoelectronics, optics, catalysis, sensors are well known [2–5].

Nowadays, plant-mediated synthesis of metal nanoparticles (MNPs) has become very important to protect the environment by increasing the use of environmentally benign solvent, reducing agent [6, 7] and replacing the use of hazardous/toxic chemical, harsh conditions or low yielding. Many natural products containing amine, carboxyl, hydroxyl and carboxylic groups are considered as candidates for non-toxic reducing agents or particle–surface stabilizers, because this functional group facilitates the formation of complexes of metal ions and then oxidizes itself to reduce metal ions to elemental metal. Hence, plant-based methods for AgNPs synthesis using the Sacha inchi oil, agricultural wastes, leaves [8–10], *Citrus sinensis* peel extract [11], edible mushroom extract [12], *Aloe vera* [13], clove extract [14] and extracts from coffees and teas [15] are widely grown in popularity.

Lantana camara L. is a woody straggling plant with various flower colors, red, pink, white, yellow and violet (Fig. 1). The plant is growing luxuriantly at elevations up to 2000 m in tropical, subtropical and temperate regions [16]. It is regarded both as a notorious weed and a popular ornamental garden plant and has found various uses in folk medicine in many parts of the world. In Central and South America, a tea prepared from the leaves and flowers was taken against fever, influenza, stomachache, chicken pox, measles, rheumatisms, asthma and high blood pressure [17, 18]. In Asian countries, leaves were used to treat cuts, rheumatisms, ulcers, leprosy and scabies and used as a vermifuge [17]. In Ghana, infusion of the whole plant was used for bronchitis and the powdered root in milk was given to children for stomachache [19]. The major phyto-constituents of *L. camara* are mono- and sesquiterpenes (bisabolene, β-curcumene, γ-curcumene, safrole), triterpenes (lantanolic and lantic acids, ursolic acid, lupane), iridoid glycosides (theveside, lamiridoside, epiloganin), flavonoids (hispidulin, glycoside camaraside, trimethoxy quercetin derivatives) [16].

Fig. 1 *Lantana camara* flower

On looking overall biological importance of *L. camara,* we are trying to explore their new application in material science. Thirumurugan et al. [20], Ajitha et al. [21] and Dash et al. [22] already reported the biosynthesis of AgNPs and gold NPs using leaf extracts of *L. camara,* due to the presence of reducing agents within their leaves. But the use of the flower extract may also be a novel alternative for this purpose. The present study describes the synthesis of AgNPs using *L. camara* flower extracts at room temperature, characterization and its applications in degradation of methylene blue (MB) and antioxidant activities. Thus, the utilization of this weed in industrial processes for the production of high-performance materials could be an additional source of revenue for farmers. However, to the best of our knowledge, *L. camara* flower has never been used to prepare AgNPs. MB is one of the well-known cationic/thiazine dyes, used in the analysis of trace levels of sulfide ions in aquatic samples. It has been widely used in dying materials for wood, silk, cotton [23], antimalarial and chemotherapeutic agent, microbiology, surgery and diagnostic field [24–26]. Though MB is not highly hazardous, but acute exposure can cause some harmful effects like increased heart rate, vomiting, shock, cyanosis, jaundice, quadriplegia and tissue necrosis in humans [27]. Thus, removal of MB from wastewater effluent is very important due to their potential toxicity to human and environment.

2 Materials and methods

2.1 Synthesis of silver nanoparticles

All chemicals were of analytical grade and used without any purification. Silver nitrate ($AgNO_3$, 99.0 %) was purchased from Spectrum (USA), and *L. camara* flowers were collected from the local garden near Universidad de las

Fuerzas Armadas, Sangolqui, Ecuador. 1,1-Diphenyl-2-picrylhydrazyl (DPPH·, >99.5 %) was purchased from Sigma-Aldrich, USA. Milli-Q water was used in all experiments. The collected fresh *L. camara* flowers (2 g) were washed thoroughly with Milli-Q water and heated (55–60 °C) in 20 mL of ethanol (95 %) for 10 min. After cooling, the yellow color extract was filtered using Whatman No. 1 paper. The filtrate was collected in 20-mL Erlenmeyer flask and stored at 4 °C for further use. For green synthesis, 2 mL of filtrate was mixed with 18 mL of 1 mM $AgNO_3$ solution at room temperature (22–25 °C). Reduction occurs rapidly as indicated by the appearance of wine red color after 30 min and studied the formation of the AgNPs at different time intervals.

2.2 Evaluation of antioxidant activity

The scavenging activity of the AgNPs at different time intervals was measured by using DPPH· as a free radical model and a method adapted from Kumar et al. [10]. An aliquot (1.0–0.2 mL) of AgNPs or control and 1.0–1.8 mL of H_2O was mixed with 2.0 mL of 0.2 mM (DPPH·) in 95 % ethanol. The mixture was vortexed vigorously and allowed to stand at room temperature for 30 min in the dark. Absorbance of the mixture was measured spectrophotometrically at 517 nm, and the free radical scavenging activity was calculated using Eq. (1):

$$\text{Scavenging effect } (\%) = [1 - \{\text{absorbance of sample/absorbance of control}\}] \times 100 \quad (1)$$

The scavenging percentage of all samples were plotted. The final result was expressed as % of DPPH· free radical scavenging activity (mL).

2.3 Evaluation of photocatalytic activity

To evaluate the photocatalytic activity of the AgNPs, degradation of MB in aqueous solution as a model system was investigated [8]. The UV light was used as direct sunlight source. 0.2–1.0 mL of AgNPs and 0.8–0.2 mL of H_2O were added to 5 mL of 10 mg/L MB solution. A control setup was also maintained without AgNPs. The dispersion was put under the sunlight (950–1050 cd/m^2). The absorbance spectrum of the solution was subsequently measured using UV–visible spectrophotometer at wavelength 664 nm for different time intervals.

2.4 Characterization of silver nanoparticles

The *L. camara* flowers-mediated AgNPs were confirmed by UV–visible, single-beam spectrophotometer (Thermo Spectronic, GENESYS^{TM} 8, England, Quartz Cell, path length 10 mm and graph plotted on the Origin 6.1 program). Size and selective area electron diffraction (SAED) pattern of nanoparticles were studied on transmission electron microscopy, TEM (FEI, Technai, G2 spirit twin, Holland). The hydrodynamic particle size distributions of nanoparticles were determined using the HORIBA, Dynamic Light Scattering (DLS) version LB-550 program. X-ray diffraction (XRD) studies on thin films of the nanoparticle were carried out using a BRUKER D8 ADVANCE brand θ–2θ configuration (generator-detector) X-ray tube copper $\lambda = 1.54$ Å and LynxEye PSD detector. The diffracted intensities were recorded from 20° to 70° 2θ angles.

3 Results and discussion

3.1 Visual and UV–Vis study

As shown in Fig. 2, the use of *L. camara* flower extract was hypothesized to be an efficient way to synthesize and stabilize AgNPs. With the addition of *L. camara* flower extract (b) to $AgNO_3$ solution (a), the color of the solution turned from pale yellow to light pink (c–e) and then to wine red (f–i) after 168 h of the reaction, which indicated the reduction of Ag^+ and formation of AgNPs. UV–visible spectroscopy is an important technique to determine the formation and stabilization of aqueous metal nanoparticles. The color change from yellow to wine red was due to the excitation of SPR. SPR is a collective oscillation of free conduction electron induced by an interacting electromagnetic field [28]. The position of the SPR band in the UV–visible spectra is sensitive to particle size, shape, local refractive index and the extent of charge transfer between the medium and the particle [29]. As shown in Fig. 3, the ethanolic *L. camara* flower extract exhibited a broad absorbance at $\lambda_{max} = 330$ nm due to the presence of mono- and sesquiterpenes, triterpenes, iridoid glycosides, flavonoids, etc. [16]. Initially, the progress of the new absorbance band at visible region, $\lambda_{max} = 480$–470 nm clearly indicates the preliminary synthesis of AgNPs. It was observed that SPR band becomes narrower and shifted toward shorter wavelength region and finally a sharp absorption peak occurs at 470 nm after 168 h of the reaction. It may likely result from varied natural capping agents coming from *L. camara* flower extracts.

3.2 TEM and SAED study

The size and morphology of the synthesized AgNPs were confirmed by TEM analysis. The obtained TEM images of the AgNPs prepared by *L. camara* flower extracts are

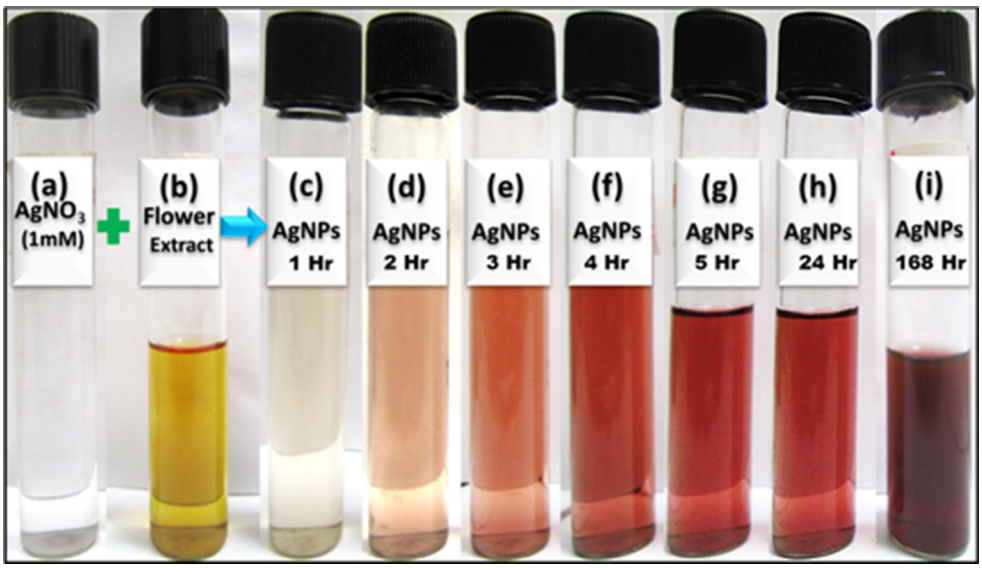

Fig. 2 *Color* change of reaction mixtures prepared by *a* 1 mM $AgNO_3$ (aq) containing and *b L. camara* flower extract at different time intervals

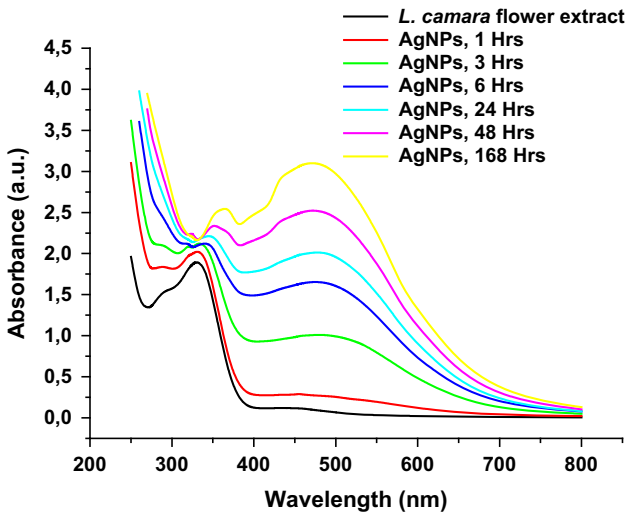

Fig. 3 UV–Vis absorbance spectra of as prepared AgNPs at different time intervals

shown in Fig. 4. It clearly indicates that the synthesized AgNPs are roughly spherical and a layer of organic material surrounding the synthesized AgNPs which may explain the good dispersion in solution exhibited by these synthesized AgNPs. The particle size was distributed in the range of 16–40 nm with a small degree of agglomeration. Further, crystalline nature of the AgNPs was confirmed by the selected area electron diffraction (SAED) pattern with bright circular spot.

3.3 DLS study

DLS measures the hydrodynamic diameter of the synthesized AgNPs, whereas the diameter observed by TEM indicates that of dried AgNPs. Figure 5 shows the size distribution histogram of the AgNPs. The particle size was distributed in the range of 20–150 nm with a mean particle size of 53.5 nm. The particle size obtained by DLS study was larger than the particle size obtained by TEM study. This is due to the ligands/phytochemicals attached to the surface of AgNPs [18, 22].

3.4 XRD study

The peaks in the X-ray diffraction pattern (Fig. 6) are due to three Bragg reflection peaks at 2θ values of 38.290°, 44.606° and 64.462° corresponding to (111), (200) and (220) planes of silver which are observed and compared with the ICSD No.: 01-087-0717. All the reflections correspond to pure silver metal with face-centered cubic symmetry [30] and confirm crystalline nature. Since that Bragg peak is wide, implying the products are in nanosize. The diameter of the synthesized AgNPs was calculated using the Scherrer equation which was around 33 ± 5 nm and was in good agreement with TEM results.

3.5 Mechanism of reduction of Ag^+ to AgNPs

The possible mechanism for the reduction of Ag^+ is proposed and shown in Fig. 7. The formation of AgNPs from Ag^+ ions is initiated by the chemical reactions in the presence of the major phytochemicals (flavonoids, mono- and sesquiterpenes, ursolic acid, iridoid glycosides, etc.) [16] present in the *L. camara* flower extract as reducing and stabilizing agents. In this scheme, Ag^+ ions can interact with O–H groups, which subsequently undergo oxidation to –CHO and –COOH forms with consequent reduction of

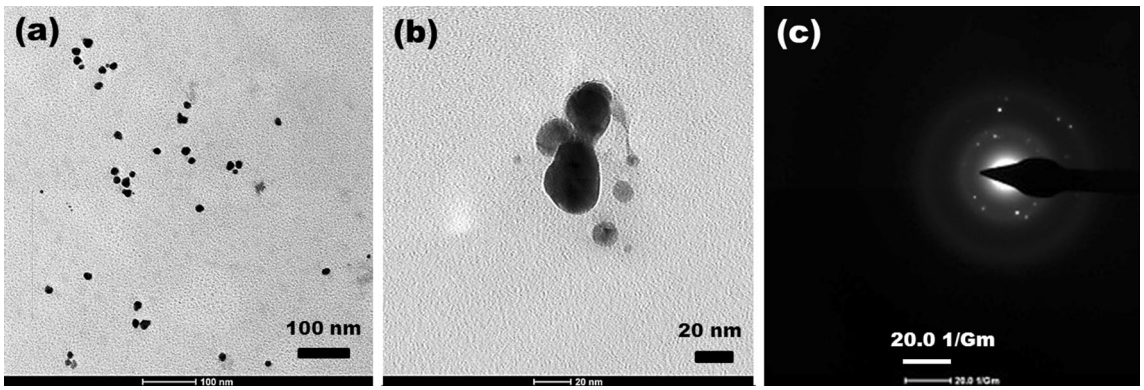

Fig. 4 TEM images of AgNPs prepared by *L. camara* flower extract

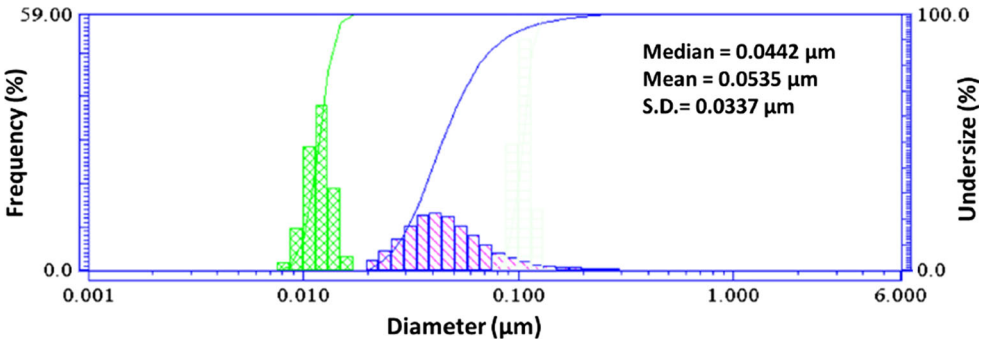

Fig. 5 DLS pattern of prepared AgNPs

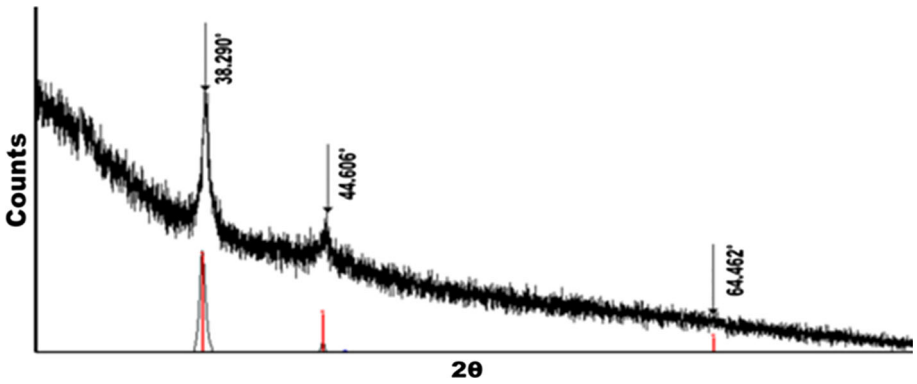

Fig. 6 XRD images of AgNPs prepared by *L. camara* flower extract

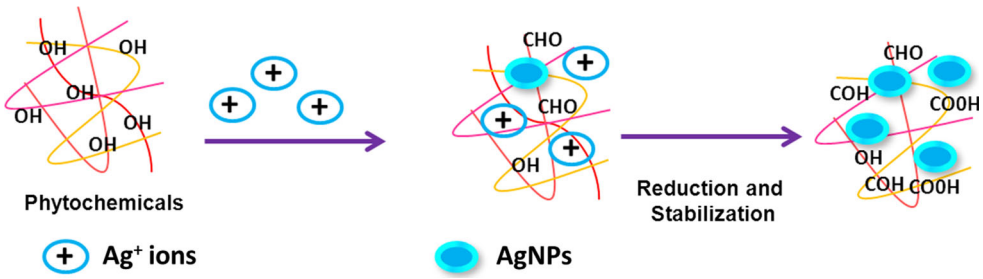

Fig. 7 Schematic diagram for biosynthesis of AgNPs using flower extract of *L. camara*

Ag^{+} to AgNPs. Finally, –COOH groups help in the stabilization of AgNPs.

3.6 Antioxidant study

DPPH· is a stable compound, and it will be reduced by accepting the hydrogen or electrons. The reducing activity of *L. camara* flower extract and AgNPs was quantified spectrophotometrically by changing the DPPH· color from purple to yellow. In the present study, percent of inhibition of DPPH· radical scavenging activity was shown in Fig. 8. It was found that the DPPH· scavenging activity of the *L. camara* flower extract was increased in a dose-dependent manner, whereas AgNPs has a slight deviation at higher dose with lapse of time. It was due to the involvement of phytochemicals for the stabilization of AgNPs. The maximum scavenging/antiradical efficacy for the *L. camara* flower extract was 87.41 % in 1 mL and for AgNPs was found to be 77.44, 69.10, 65.60, 68.69, 66.32, 63.11, 61.76 % at 1, 2, 3, 4, 5, 48, 168 h in 0.8 mL/0.2 mM. The antioxidant efficacy may be due to encapsulation of bioactive molecules on the spherical surface of AgNPs through the electrostatic attraction between negatively charged bioactive compounds (COO^{-}, O^{-}) and neutral or positively charged nanoparticles [10, 31]. The effect of activity depends on the site of attachment of the metals and its consequent impact on the activity of the antioxidant agent.

3.7 Photocatalytic effect

Besides the optical properties, AgNPs have excellent catalytic activity. Generally, it is accepted that chemistry changes with size [9]. The role of metal nanoparticle as an electron transfer catalyst is thus expected to vary with size. The characteristic absorption peak at 664 nm of MB dye was used for monitoring the catalytic degradation process [8]. The rate of MB decomposition catalyzed by AgNPs is assumed to be fitted by a first-order rate law [32] which shows a linear relationship between ln (At/Ao) and reaction time and the slope gives the negative rate constant in each case. The rate constant (k) of photocatalytic degradation of MB dye was investigated at different time intervals in the presence of different quantities (0.2–1.0 mL) of AgNPs, and the rate constant that was evaluated from the slope of the straight line is shown in Fig. 9a. From the study, it revealed that the rate constant was increased gradually ($k_5 < k_4 < k_3 < k_2 < k_1$) with increasing the concentration of AgNPs, due to increase in the surface area of the active site of AgNPs. The rate constant was found to be higher ($k_1 = 3.40736 \times 10^{-3}$ min^{-1}), when 1 mL of AgNPs was used in the photocatalytic degradation reaction. Figure 9b shows the main MB absorption peak at 664 nm, decreased gradually with the extension of the exposure time, indicating the optimized photocatalytic degradation, 70.20 %, 10 mg/L dye of MB in 6 h. Decrease in the absorption

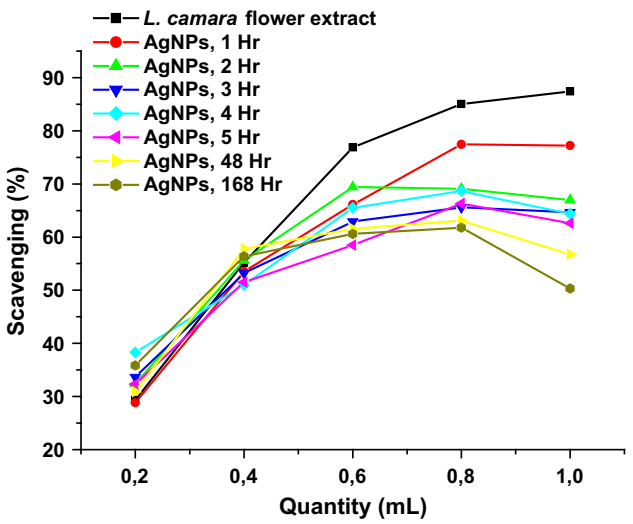

Fig. 8 Antioxidative properties *L. camara* flower extract and AgNPs at different time intervals

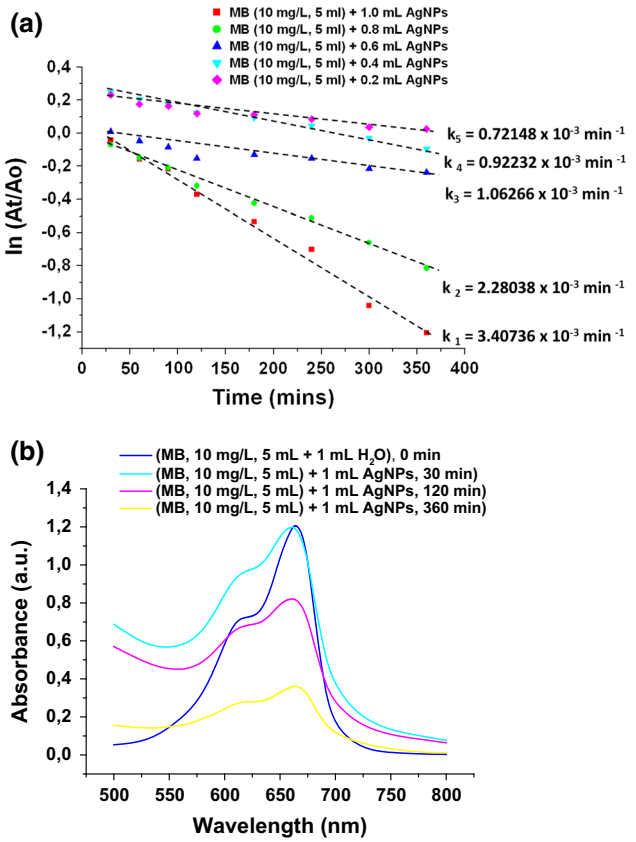

Fig. 9 **a** Kinetic plot of ln (At/Ao) vs. time and **b** optimized photocatalytic pattern of AgNPs for degradation of MB

intensity of the band at λ_{max} during the irradiation also expresses the loss of the conjugation of the organic molecule, MB. When the reaction is carried out under sunlight using glass tubes (glass is opaque to UV light), the degradation activity increased drastically.

4 Conclusions

The current study shows the utilization of *L. camara* flower extract as both the reducing and stabilizing agent in the ecofriendly synthesis of AgNPs. UV–visible spectroscopy, TEM, DLS and XRD analysis confirmed that the AgNPs are spherical, crystalline and 33 ± 5 nm average sized. The formed AgNPs exhibited more than 70 % degradation of MB in sunlight for 6.0 h. In addition, the surface-modified AgNPs clearly demonstrated significant antioxidant activity ($\geq$60 % for 0.2 mM) against DPPH· and could be used effectively in future biotechnology concerns.

Acknowledgments This scientific work has been funded by the Prometeo Project of the National Secretariat of Higher Education, Science, Technology and Innovation (SENESCYT), Ecuador. We thank Dr. Alexis Debut, ESPE, and Dr. Colon Velasquez (Director, INIGEMM, Ecuador) for providing TEM and XRD instrumental facility.

Compliance with ethical standards

Conflict of interest The authors declare that there is no conflict of interests regarding the publication of this article.

References

1. Sun Y, Xia Y (2002) Shape controlled synthesis of gold and silver nanoparticles. Science 298:2176–2179
2. Nam J, Won N, Jin H, Chung H, Kim S (2009) pH-induced aggregation of gold nanoparticles for photothermal cancer therapy. J Am Chem Soc 131(38):13639–13645
3. Narayanan KB, Sakthivel N (2011) Synthesis and characterization of nano-gold composite using *Cylindrocladium floridanum* and its heterogeneous catalysis in the degradation of 4-nitrophenol. J Hazard Mater 189:519–525
4. Li J, Chen X, Ai N, Hao J, Chen Q, Strauf S et al (2011) Silver nanoparticle doped TiO_2 nanofiber dye sensitized solar cells. Chem Phys Lett 514:141–145
5. Fayaza AM, Girilal M, Mahdy SA, Somsundar SS, Venkatesan R, Kalaichelvan PT (2011) Vancomycin bound biogenic gold nanoparticles: a different perspective for development of anti VRSA agents. Process Biochem 46:636–641
6. Raveendran P, Fu J, Wallen SL (2003) Completely "green" synthesis and stabilization of metal nanoparticles. J Am Chem Soc 125(46):13940–13941
7. Thakkar KN, Mhatre SS, Parikh RY (2010) Biological synthesis of metallic nanoparticles. Nanomedicine 6(2):257–262
8. Kumar B, Smita K, Cumbal L, Debut A (2014) Sacha inchi (*Plukenetia volubilis* L.) oil for one pot synthesis of silver nanocatalyst: an ecofriendly approach. Ind Crops Prod 58:238–243
9. Kumar B, Smita K, Cumbal L, Debut A (2014) Sacha inchi (*Plukenetia volubilis* L.) shell biomass for synthesis of silver nanocatalyst. J Saudi Chem Soc. doi:10.1016/j.jscs.2014.03.005
10. Kumar B, Smita K, Cumbal L, Debut A (2014) Synthesis of Silver Nanoparticles using Sacha inchi (*Plukenetia volubilis* L.) leaf extracts. Saudi J Biol Sci 21(6):605–609
11. Kaviya S, Santhanalakshmi J, Viswanathan B, Muthumary J, Srinivasan K (2011) Biosynthesis of silver nanoparticles using *Citrus sinensis* peel extract and its antibacterial activity. Spectrochim Acta Part A 79:594–598
12. Philip D (2009) Biosynthesis of Au, Ag, and Au-Ag nanoparticles using edible mushroom extract. Spectrochim. Acta Part A 73:374–381
13. Chandran SP, Chaudhary M, Pasricha R, Ahmad A, Sastry M (2006) Synthesis of gold nanotriangles and silver nanoparticles using *Aloe vera* plant extract. Biotechnol Prog 22:577–583
14. Vijayaraghavan K, Kamala Nalini SP, Prakash NU, Madhankumar D (2012) Biomimetic synthesis of silver nanoparticles by aqueous extract of *Syzygium aromaticum*. Mater Lett 75:33–35
15. Nadagouda MN, Varma RS (2008) Green synthesis of silver and palladium nanoparticles at room temperature using coffee and tea extract. Green Chem 10:859–862
16. Ghisalberti EL (2000) *Lantana camara* L. (Verbenaceae). Fitoterapia 71:467–486
17. Ross IA (1999) Medicinal plants of the world. Chemical constituents, traditional and modern medical uses. Humana Press, New Jersey
18. Kumar B, Smita K, Cumbal L, Debut A (2015) *Lantana camara* berry for the synthesis of silver nanoparticles. Asian Pac J Trop Biomed 5(3):192–195
19. Irvine FR (1961) Woody plants of Ghana. Oxford University Press, London
20. Thirumurugan A, Neethu AT, Hema PK, Prakash P (2011) Biological synthesis of silver nanoparticles by *Lantana camara* leaf extracts. Int J Nanomater Biostruct 1(2):22–24
21. Ajitha B, Reddy YAK, Reddy PS (2015) Green synthesis and characterization of silver nanoparticles using *Lantana camara* leaf extract. Mater Sci Eng C 49:373–381
22. Dash SS, Bag BG, Hota P (2014) *Lantana camara* Linn leaf extract mediated green synthesis of gold nanoparticles and study of its catalytic activity. Appl Nanosci. doi:10.1007/s13204-014-0323-4
23. Hameed BH, Din ATM, Ahmad AL (2007) Adsorption of methylene blue onto bamboo-based activated carbon: kinetics and equilibrium studies. J Hazard Mater 141:819–825
24. Small JM, Hintelmann H (2007) Methylene blue derivatization then LC-MS analysis for measurement of trace levels of sulfide in aquatic samples. Anal Bioanal Chem 387:2881–2886
25. Burhenne J, Riedl KD, Rengelshausen J, Meissner P, Muller O, Mikus G et al (2008) Quantification of cationic antimalaria agent methylene blue in different human biological matrices using cation exchange chromatography coupled to tandem mass spectrometry. J Chromatogr B 863:273–282
26. Xu JZ, Dai L, Wu B, Ding T, Zhu JJ, Lin H et al (2009) Determination of methylene blue residues in aquatic products by liquid chromatography-tandem mass spectrometry. J Sep Sci 32:4193–4199
27. Kumar B, Smita K, Cumbal L, Debut A (2015) Ultrasound agitated phytofabrication of palladium nanoparticles using Andean blackberry leaf and its photocatalytic activity. J Saudi Chem Soc 19:574–580
28. Kahrilas GA, Wally LM, Fredrick SJ, Hiskey M, Prieto AL, Owens JE (2014) Microwave-assisted green synthesis of silver nanoparticles using orange peel extract. ACS Sustain Chem Eng 2(3):367–376

29. Aromal SA, Philip D (2012) Green synthesis of gold nanoparticles using *Trigonella foenum-graecum* and its size-dependent catalytic activity. Spectrochim Acta Part A Mol Biomol Spectrosc 97:1–5
30. Kumar B, Smita K, Cumbal L, Debut A, Pathak RN (2014) Sonochemical synthesis of silver nanoparticles using starch: a comparison. Bioinorg Chem Appl 2014:1–8. doi:10.1155/2014/784268
31. Kumar B, Smita K, Cumbal L, Angulo Y (2015) Fabrication of silver nanoplates using *Nephelium lappaceum* (Rambutan) peel: a sustainable approach. J Mol Liq 211:476–480
32. Kumar B, Smita K, Cumbal L, Debut A (2014) Green approach for fabrication and applications of zinc oxide nanoparticles. Bioinorg Chem Appl 2014:1–7. doi:10.1155/2014/523869